Electronic Supplementary Material (ESI) for Polymer Chemistry

Supporting Information for:

Synthesis by Nitroxide-Mediated Aqueous Dispersion Polymerization, Characterization, and Physical Core-Crosslinking of pH- and Thermoresponsive Dynamic Diblock Copolymer Micelles

Guillaume Delaittre,[†] Maud Save,[‡] Marianne Gaborieau,[¤] Patrice Castignolles,[¶] Jutta Rieger,[§] Bernadette Charleux*[¥]*

† Preparative Macromolecular Chemistry, Institut für Technische Chemie und Polymerchemie, Karlsruhe Institute of Technology (KIT), Engesserstr.18, 76128 Karlsruhe, Germany.

‡ IPREM Equipe de Physique et Chimie des Polymères, UMR 5254 CNRS, Université de Pau et des Pays de L'Adour, Hélioparc, 2 Avenue du Président Angot, 64053 Pau Cedex, France.

¤ University of Western Sydney, Nanoscale Organisation and Dynamics Group, School of Science and Health, Campbelltown Campus, Building 21, Locked Bag 1797, Penrith NSW 2751, Australia

¶ University of Western Sydney, School of Science and Health, Australian Centre for Research on Separation Science (ACROSS), Parramatta Campus, Locked Bag 1797, Penrith NSW 2751, Australia.

§ UPMC Univ. Paris 6, Sorbonne Universités and CNRS, Laboratoire de Chimie des Polymères, UMR 7610, 3 rue Galilée, 94200 Ivry, France.

¥ Université de Lyon, Univ Lyon 1, CPE Lyon, CNRS, UMR 5265, C2P2 (Chemistry, Catalysis, Polymers & Processes), Team LCPP Bat 308F, 43 Bd du 11 novembre 1918, 69616 Villeurbanne, France.

Mark-Houwink-Sakurada parameters of PMMA in DMF/LiBr

No Mark-Houwink-Sakurada parameters are available for PMMA in DMF/LiBr at 60 °C in the literature. A number of M_w and [η] values have however been determined in pure DMF at different temperatures ranging from 10 to 60 °C (see Table S1). We compared the values of

intrinsic viscosity and molecular weight. One set of value is a clear outlier (last line of Table S1).

Table S1. Viscosity properties (intrinsic viscosity, [η], and weight-average molecular weight, M_w) of PMMA in DMF measured at different temperatures T.

M_w (g/mol)	[η] (dL/g)	T (°C)	Determination method	Reference
82,600	0.297	25	Offline static light scattering and Ubelhode viscometer in dried DMF under nitrogen	1
124,000	0.39			
173,000	0.45			
202,000	0.517			
287,000	0.61			
360,000	0.77			
527,000	0.955			
1100,000	1.62			
17,500,000	7.7			
18,600,000	8.77			
22,700,000	9.62			
23,800,000	9.98			
17,500,000	7.7	25	Offline static light scattering and viscometer	2
18,600,000	8.77			
22,700,000	9.62			
23,800,000	9.98			
9,513,000	3.32	25	Offline static light scattering and Ubelhode viscometer	3
10,961,000	3.66			
12,175,000	3.981			
15,998,000	4.551			
15,923,000	4.657			
23,175,000	5.7676			
9,513,000	3.32			
64,368	0.233	60	?	Viscotek
714,000	0.887	10	Offline static light scattering and	4
606,000	0.813			

547,000	0.753		Ubelhode viscometer	
485,000	0.684			
319,000	0.561			
220,000	0.428			
87,000	0.255			
714,000	0.99	30		
606,000	0.894			
547,000	0.821			
485,000	0.729			
319,000	0.607			
220,000	0.465			
87,000	0.26			
714,000	1.041	50		
606,000	0.966			
547,000	0.872			
485,000	0.771			
319,000	0.635			
220,000	0.492			
87,000	0.274			
550,000	0.815	15	Offline static light scattering and Ubelhode viscometer	5
420,000	0.692			
300,000	0.533			
80,000	0.214			
550,000	0.89	25		
420,000	0.73			
300,000	0.567			
80,000	0.223			
550,000	0.919	35		
420,000	0.768			
300,000	0.6			
80,000	0.229			
550,000	0.979	45		
420,000	0.805			

300,000	0.624			
80,000	0.235			
420,000	0.837	55		
300,000	0.646			
80,000	0.249			
40,500	0.005	60	?+viscosimeter	[6]

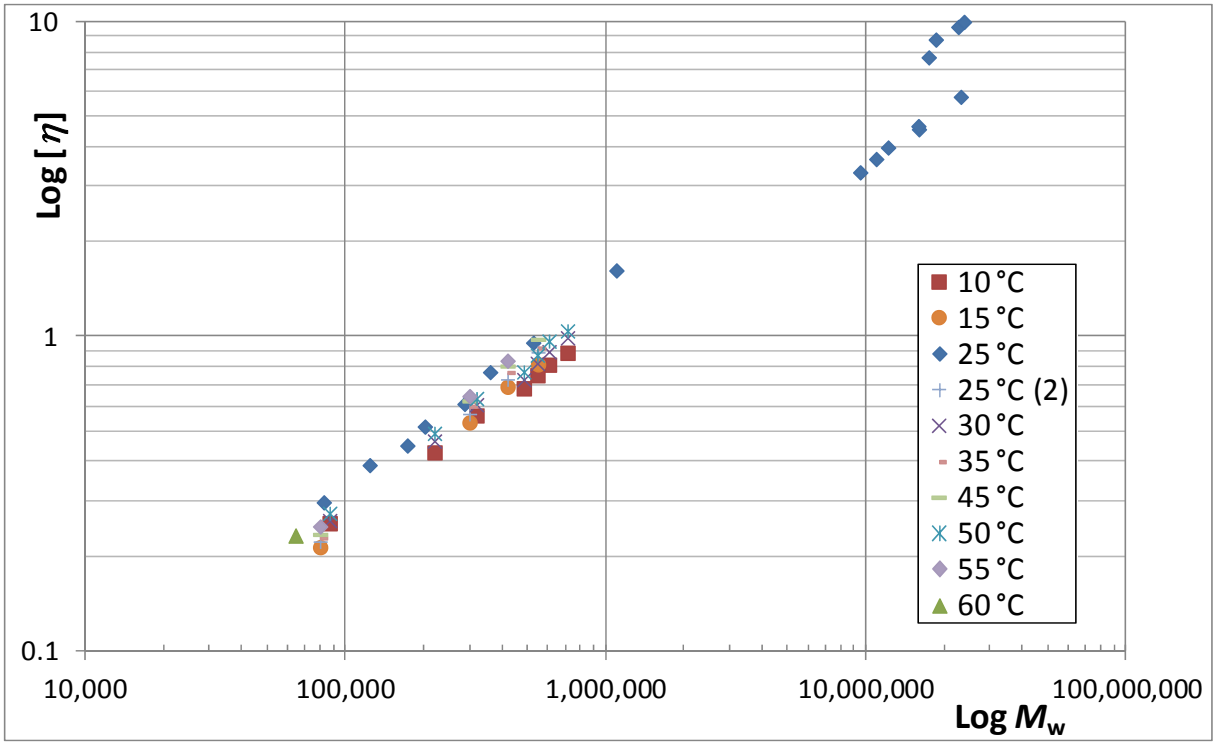

Figure S1. Mark-Houwink-Sakurada plot for PMMA in DMF measured at different temperatures (see references in Table S1 for the different literature values).

All other values given in the literature are consistent (see Figure S1). Values at 55 °C and 60 °C were plotted and fitted together (Figure S-2) to obtain the following equation:

$$\text{Log } [\eta] = 0.6961 \log M_w - 3.9979 \qquad (1)$$

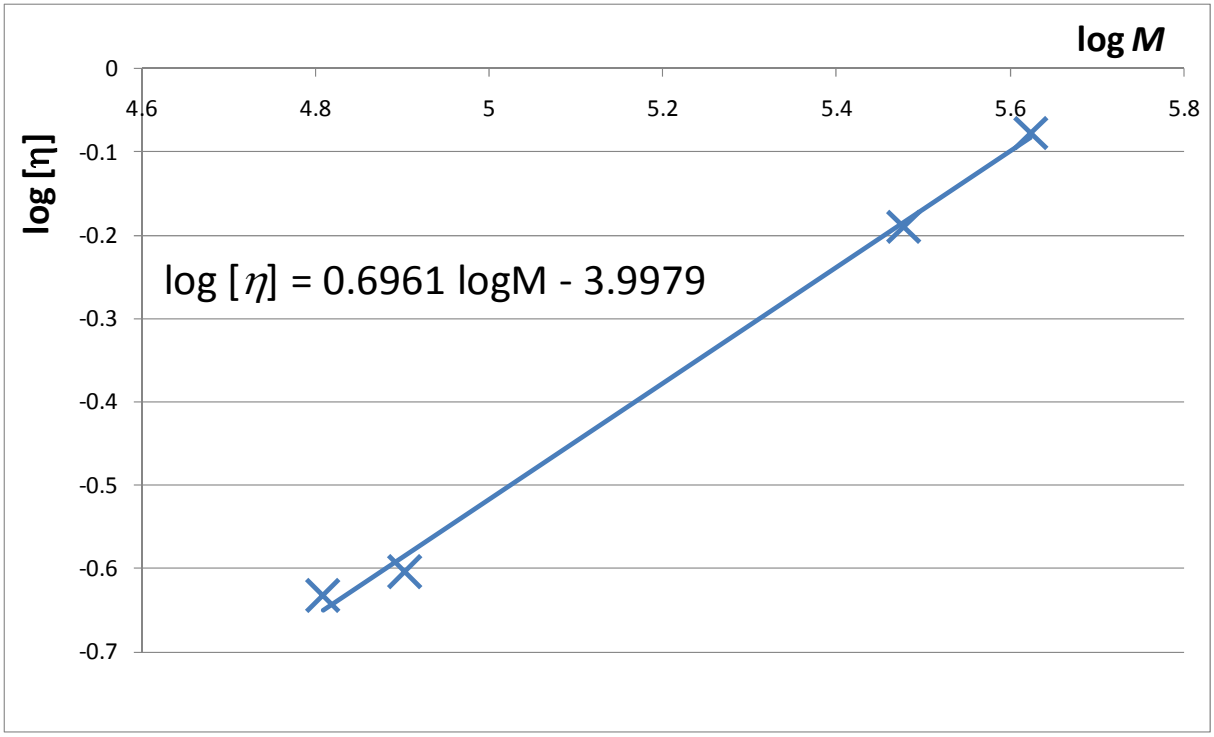

Figure S2. Mark-Houwink-Sakurada plot for PMMA in DMF measured at 55-60 °C.

Universal calibration in our SEC system

Polystyrene standards lead to a universal calibration significantly different from the PMMA one (Figure S3). Polystyrene has too low a polarity compared to the one of the stationary phase and eluents and likely adsorbs as already observed.[7] Polystyrene is certainly not separated by a size-exclusion mechanism with the Mixed C column in DMF. The universal calibration curve was thus built only with PMMA standards.

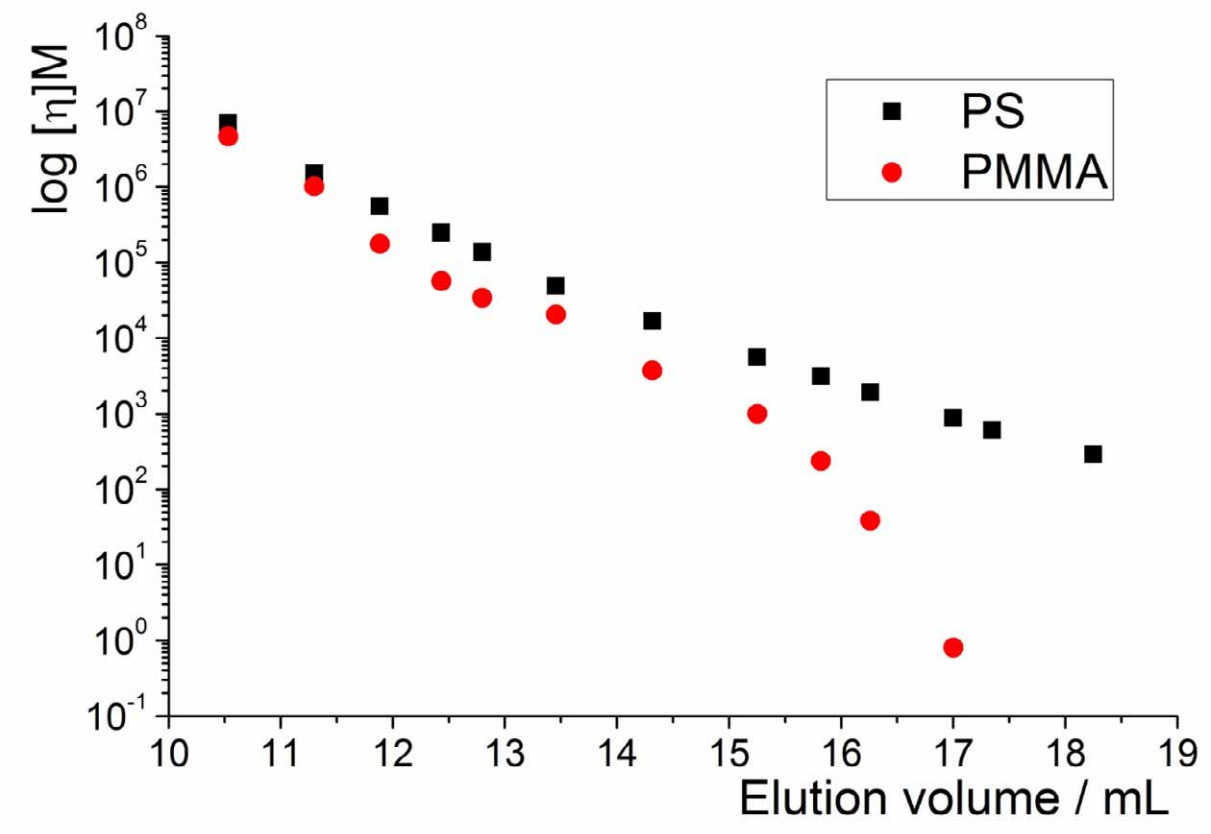

Figure S3. Comparison of the universal calibration curves obtained with polystyrene (black squares) and poly(methyl methacrylate) (red circles).

SEC Chromatograms

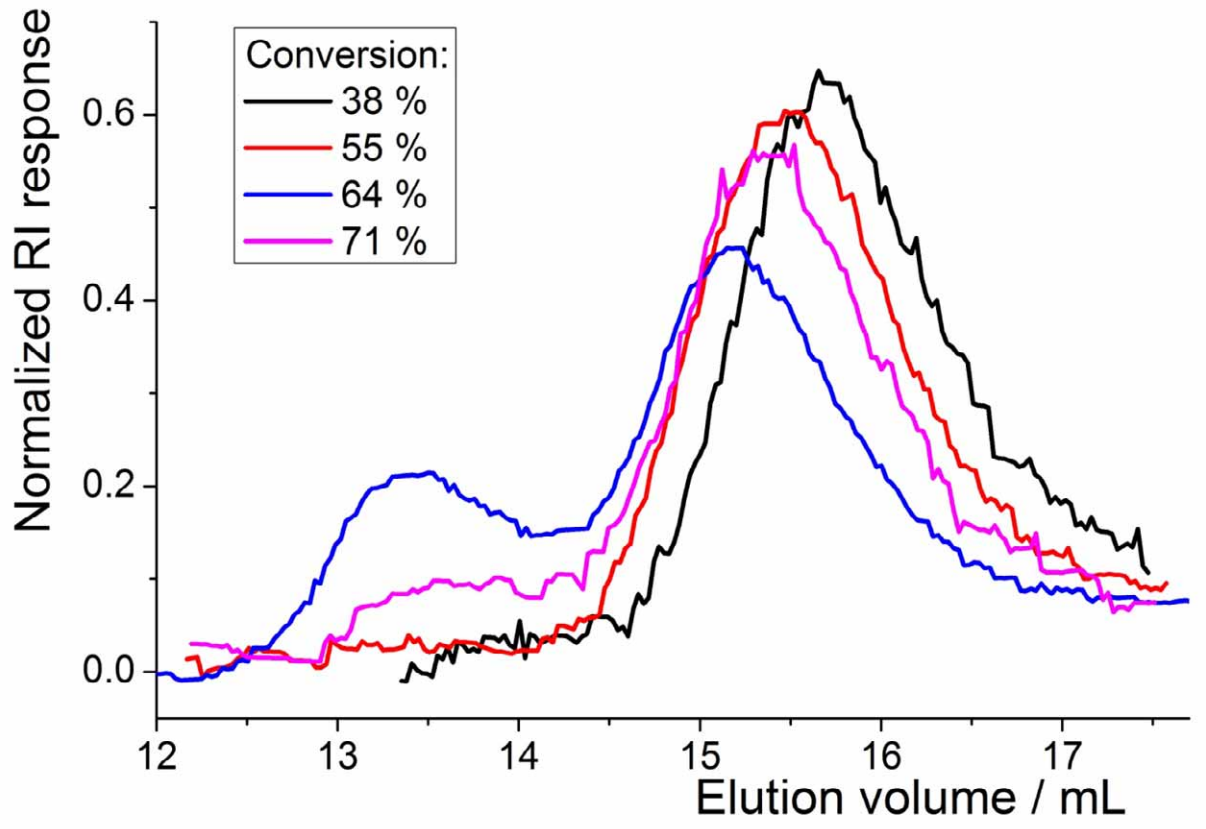

Figure S4. Chromatograms obtained by SEC/DMF of PAA-*b*-PDEAAm synthesized by dispersion polymerization of DEAAm initiated by PAA_{23}-SG1 at 112 °C (exp. 7).

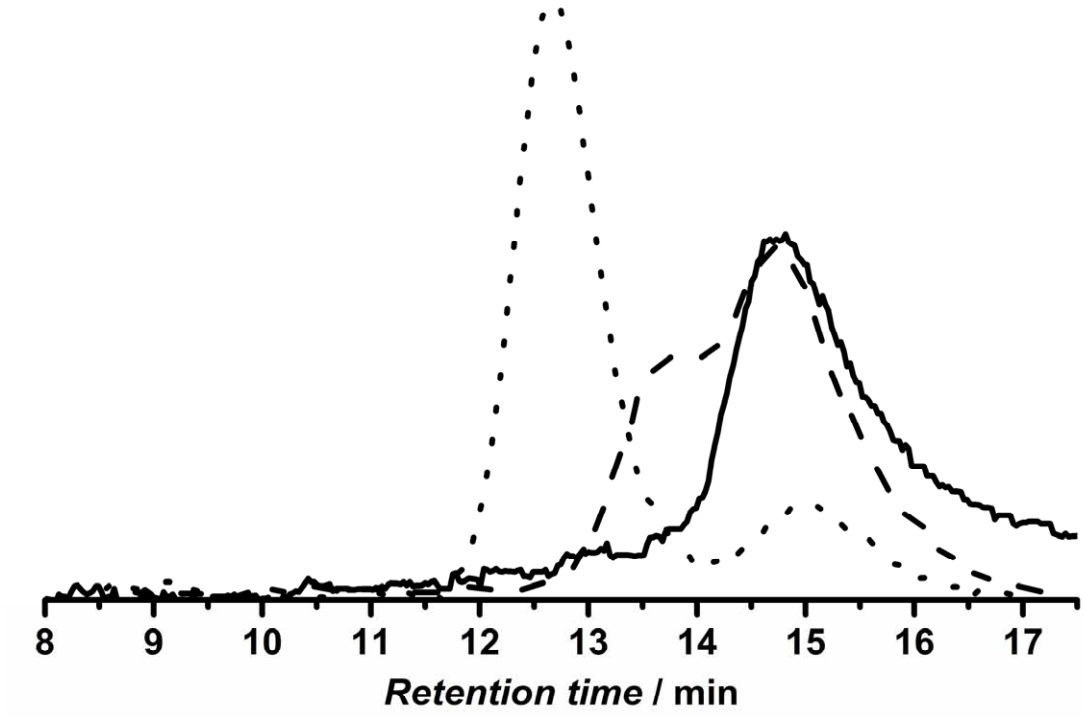

Figure S5. Chromatograms obtained by SEC/DMF of PAA-*b*-PDEAAm synthesized by dispersion polymerization of DEAAm initiated by PAA_{23}-SG1 after different treatments [acidification and drying on Mg_2SO_4 (dotted line); acidification and methylation (dashed line); and randomly obtained non-aggregated sample (solid line)].

Hydrodynamic volume distributions (HVDs)

HVDs can be determined from the raw bimodal refractometer signal, without deconvolution, using the equation below:[8]

$$w(\log V_h) = V_h W(V_h) = \left. \frac{S^*_{DRI}(t_{el})}{\frac{d \log V_h}{d\tilde{t}_{el}(V_h)}} \right|_{\tilde{t}_{el}(V_h)=t_{el}}$$

where V_h is the hydrodynamic volume, $w(\log V_h)$ is the SEC hydrodynamic volume distribution, $W(V_h)$ is the weight hydrodynamic volume distribution, $S^*_{DRI}(t_{el})$ is the refractometer signal at the elution time t_{el}, and $d\log V_h/dt_{el}(V_h)$ is the value of the derivative of the universal calibration curve at the hydrodynamic volume V_h.

HVDs are presented on Figures S6 and S7. Figure S7 shows that the aggregate peak represent a very small proportion of the total sample in terms of weight or number. However, this

weight distribution exhibits a low signal-to-noise ratio for the polymer peak and can thus not be used for comparison purposes.

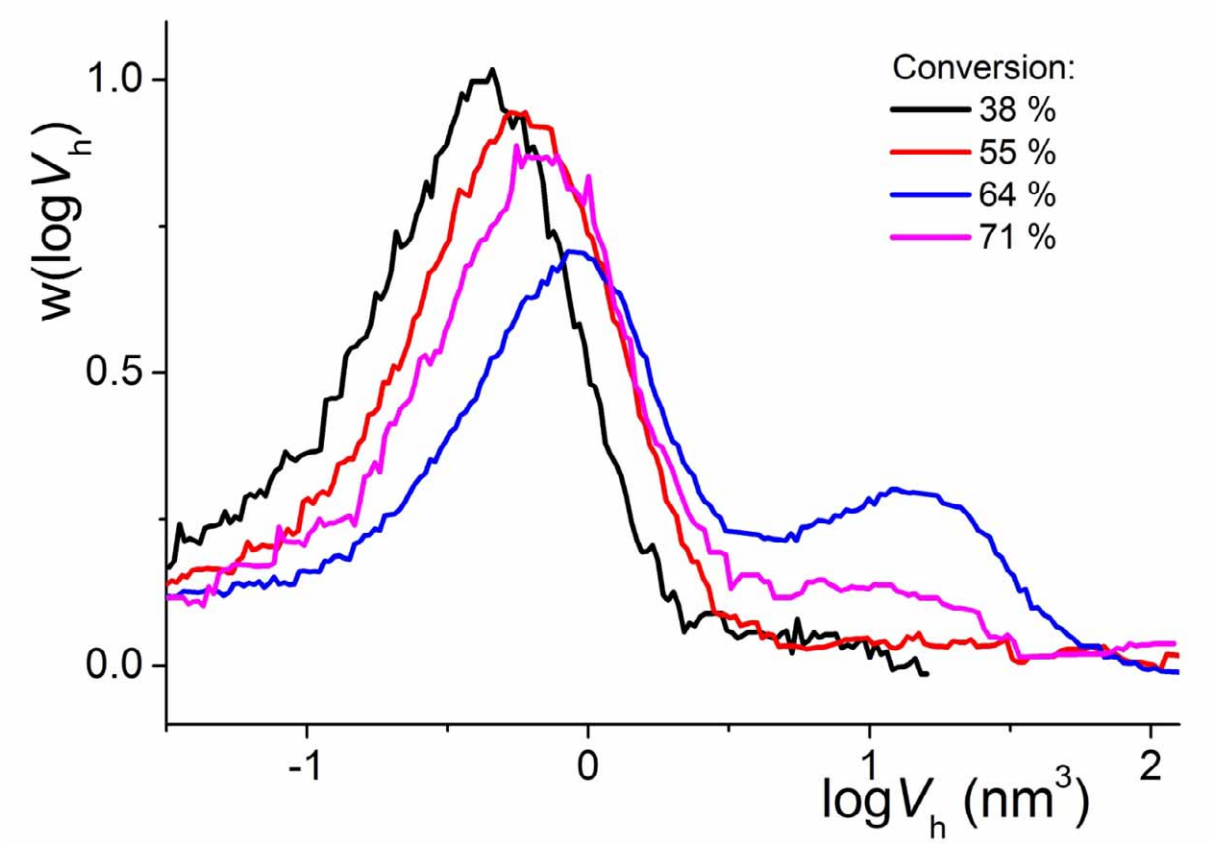

Figure S6. SEC hydrodynamic volume distributions (w(log V_h)) calculated from the chromatograms presented in Figure S4 (exp. 7).

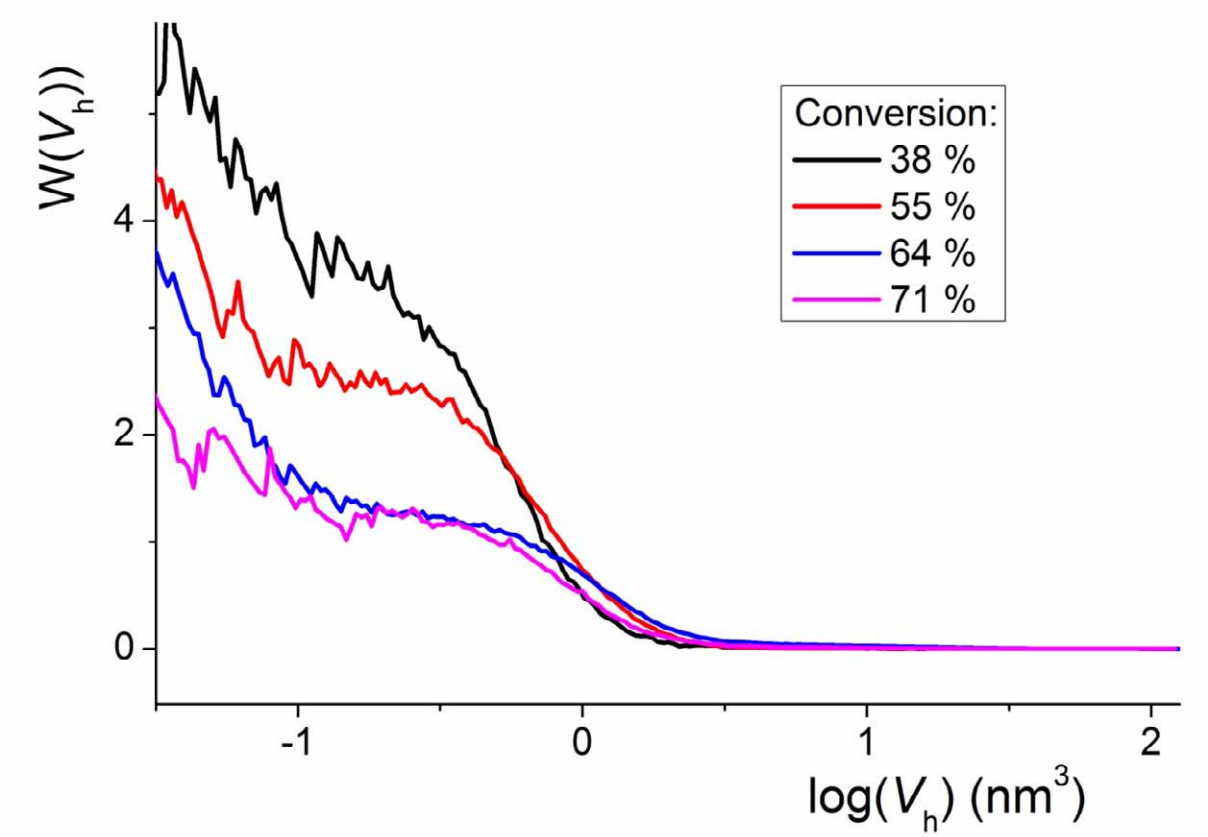

Figure S7. Weight hydrodynamic volume distributions (W(V_h)) calculated from the SEC distributions presented in Figure S4 (exp. 7).

Deconvolution

The deconvolution of the data corresponding to Figure S4, S6, and S7 is presented on Figure S8 in the case of Gaussian functions. This deconvolution is easily performed using the "multiple peaks" function of the software Origin (OriginLab). The sum of the two deconvoluted peaks poorly represents the original distribution, especially in terms of baseline. The problem is also observed when the deconvolution is done on the chromatogram (data not shown).

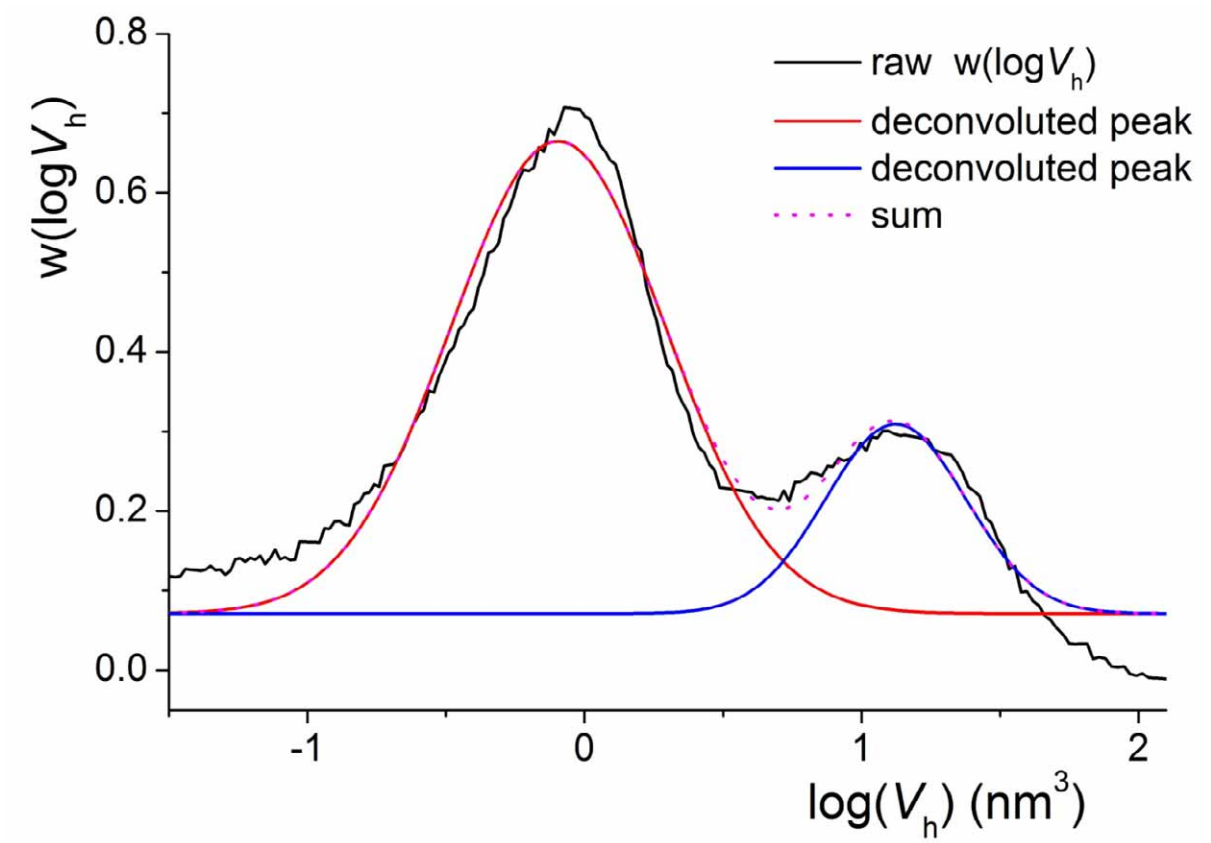

Figure S8. Deconvolution of Figure S4 (64 % conversion) using multiple Gaussian peaks.

The first issue with the deconvolution is that part of the low molecular weight tail is missing. Incomplete separation of oligomers and system peaks is a common limitation of SEC, especially recognized to lead to poor accuracy of number-average molecular weights (M_n)[9,10]. The fact that the low-molecular weight tail is missing is also an issue for the deconvolution. To obtain the correct baseline after deconvolution, we have substituted system peaks eluting after the calibration curve (PMMA-equivalent molecular weight inferior to 200 g/mol) by a perfect baseline: 200 points have been added for elution volumes between 18 and 20 mL with a RI response of 0. The large error in baseline is then significantly reduced. The sum of the two deconvoluted peaks still fits poorly the overall hydrodynamic distribution (Figure S9) or chromatogram (data not shown).

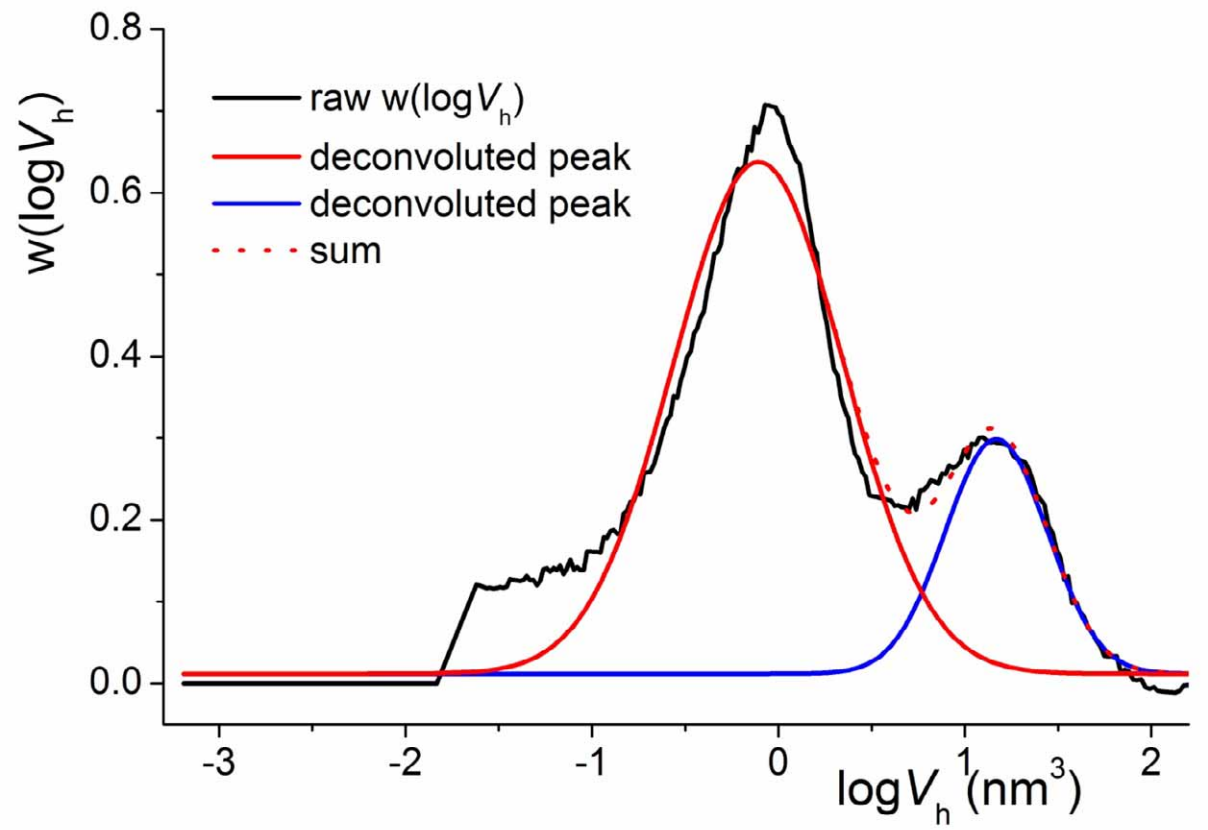

Figure S9. Same deconvolution as Figure S8 after addition of 200 "0" points.

These data were then deconvoluted using exponentially modified Gaussians. The software PeakFit (Jandel) was used for that purpose. The sum of the two deconvoluted peaks is clearly fitting better by simple visual inspection of both the chromatogram (Figure S-9) and the hydrodynamic volume distribution w(log V_h) (Figure S-10). The fit leads to visually the same results with or without addition of "zero" and the addition was thus not performed using PeakFit (data not shown).

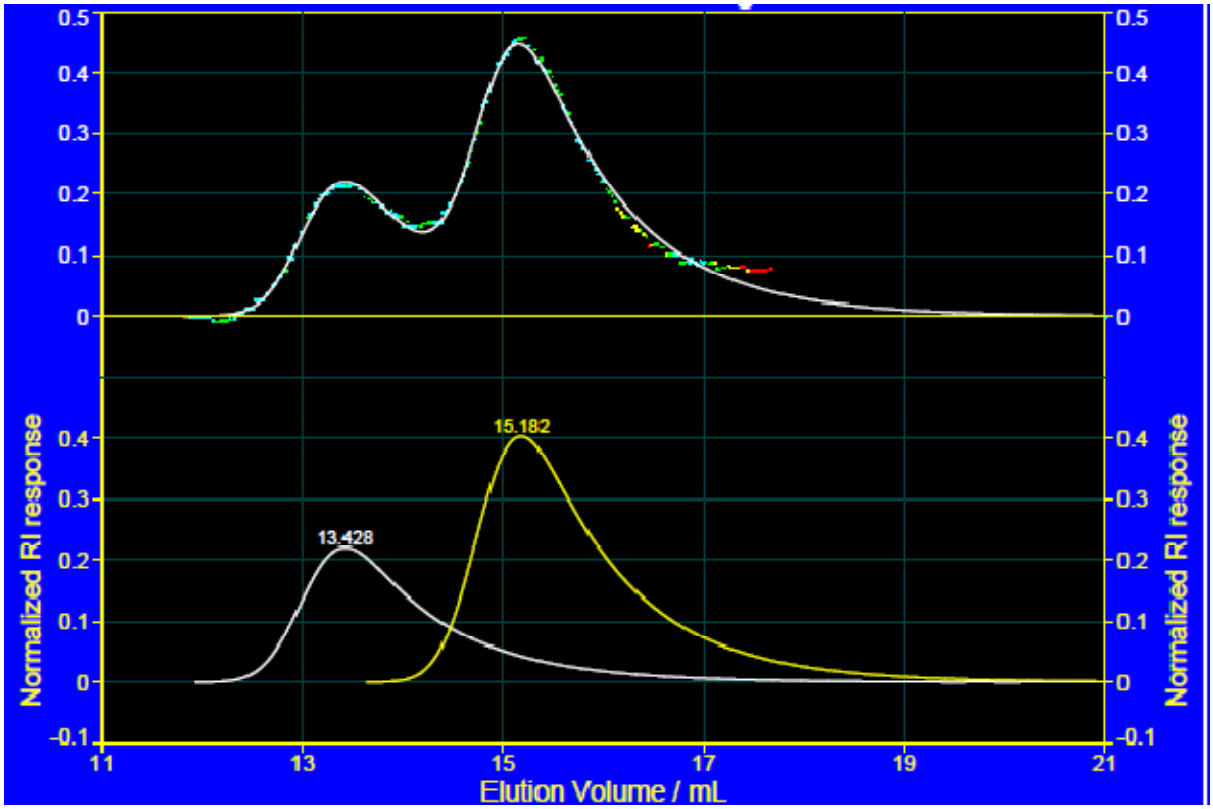

Figure S10. Deconvolution of the chromatogram presented in Figure S4 (conversion 64 %) using PeakFit: deconvoluted peaks (bottom) and sum (top, full line) compared to raw chromatogram (top, dotted line).

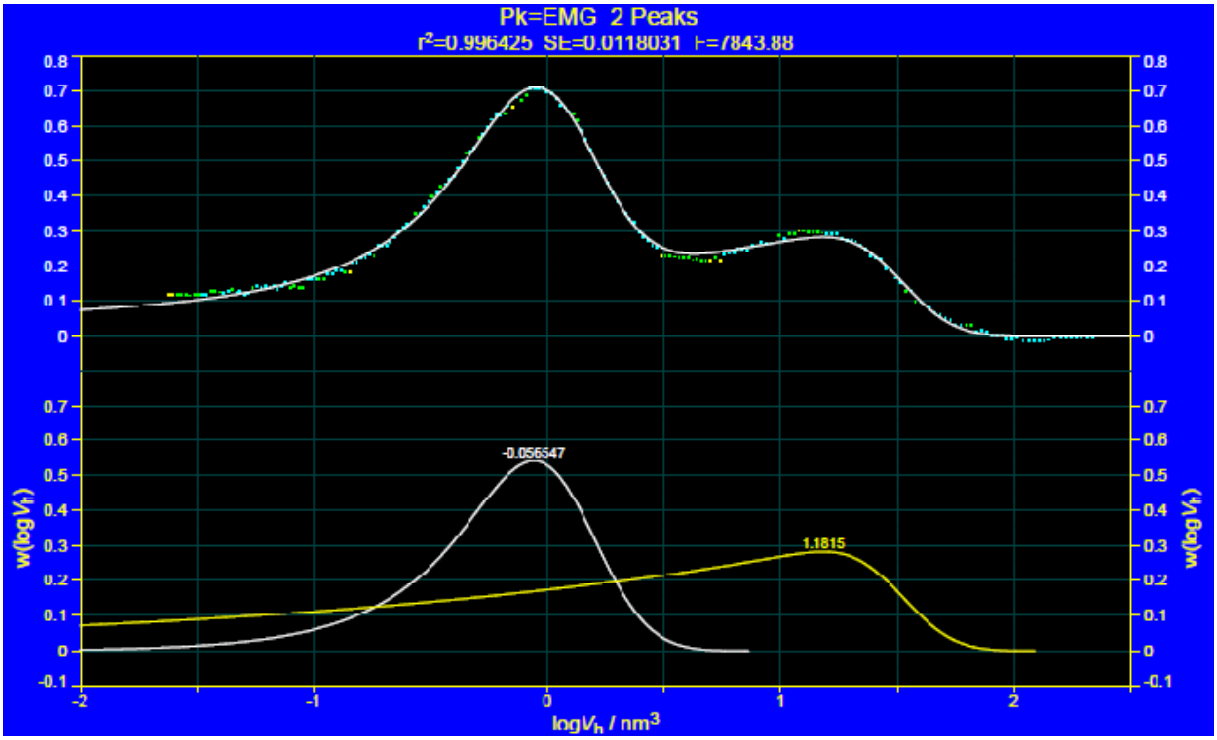

Figure S11. Deconvolution of the hydrodynamic volume distribution presented in Figure S6 (64% conversion) using PeakFit: deconvoluted peaks (bottom) and sum (top, full line) compared to raw chromatogram (top, dotted line). Note that this distribution corresponds to the chromatogram presented on Figure S10.

It is important to note that the deconvolution of the hydrodynamic volume distribution leads in the oligomers range to a higher proportion of aggregates than free polymer chains. This is physically impossible. Furthermore, the two types of deconvolutions lead to different results when the hydrodynamic volume distributions are compared (Figure S12). The deconvolutions were thus performed on the raw chromatograms before calculating the hydrodynamic volume distribution corresponding to the polymer peak.

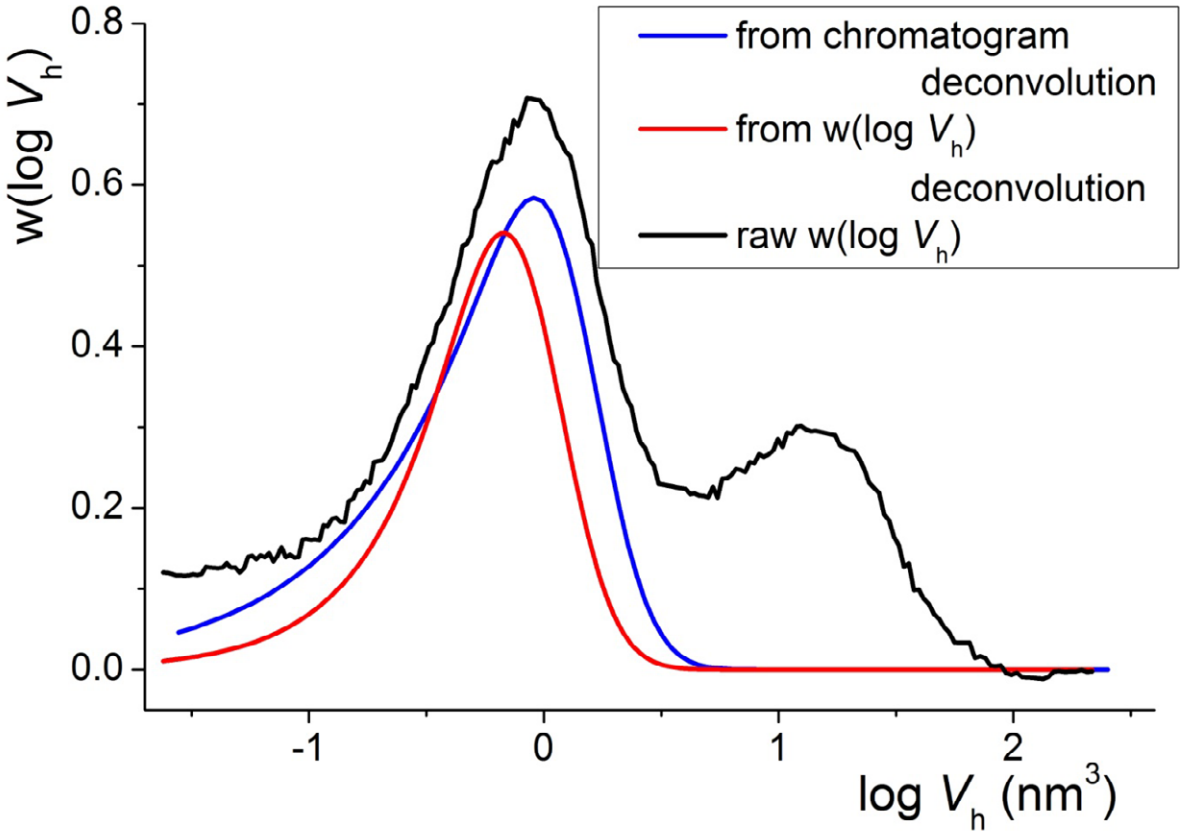

Figure S12. Comparison of the raw w(log Vh) distribution (black line) with w(log Vh) corresponding to the polymeric unimers obtained from deconvolution of the w(log Vh) (red line) or from deconvolution of the chromatogram (blue line).

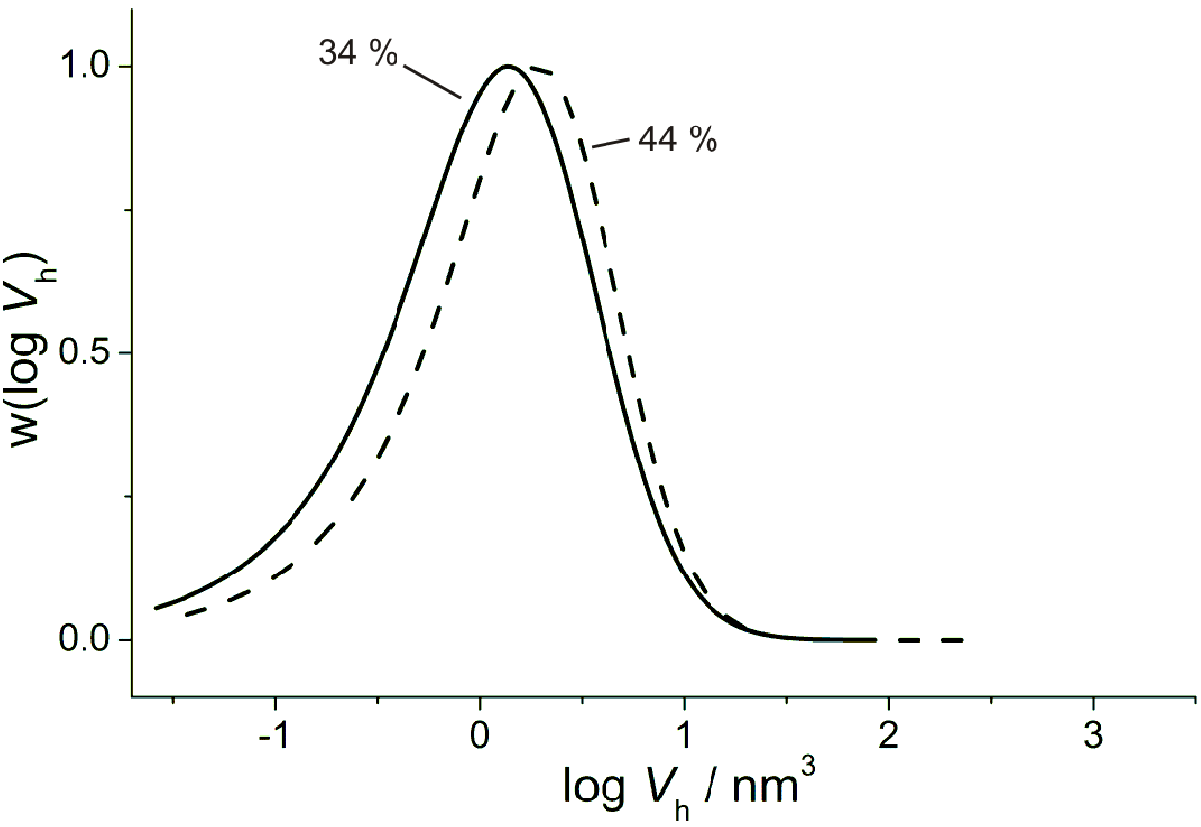

Figure S13. Overlay of hydrodynamic volume distributions at two monomer conversions for the dispersion polymerization of DEAAm initiated by PAA_{23}-SG1 at 112 °C, $[PAA\text{-}SG1]_0$ = 7.3×10^{-3} mol L_{aq}^{-1}, 20 wt.% solids, and r = 0.05 (Exp. 3).

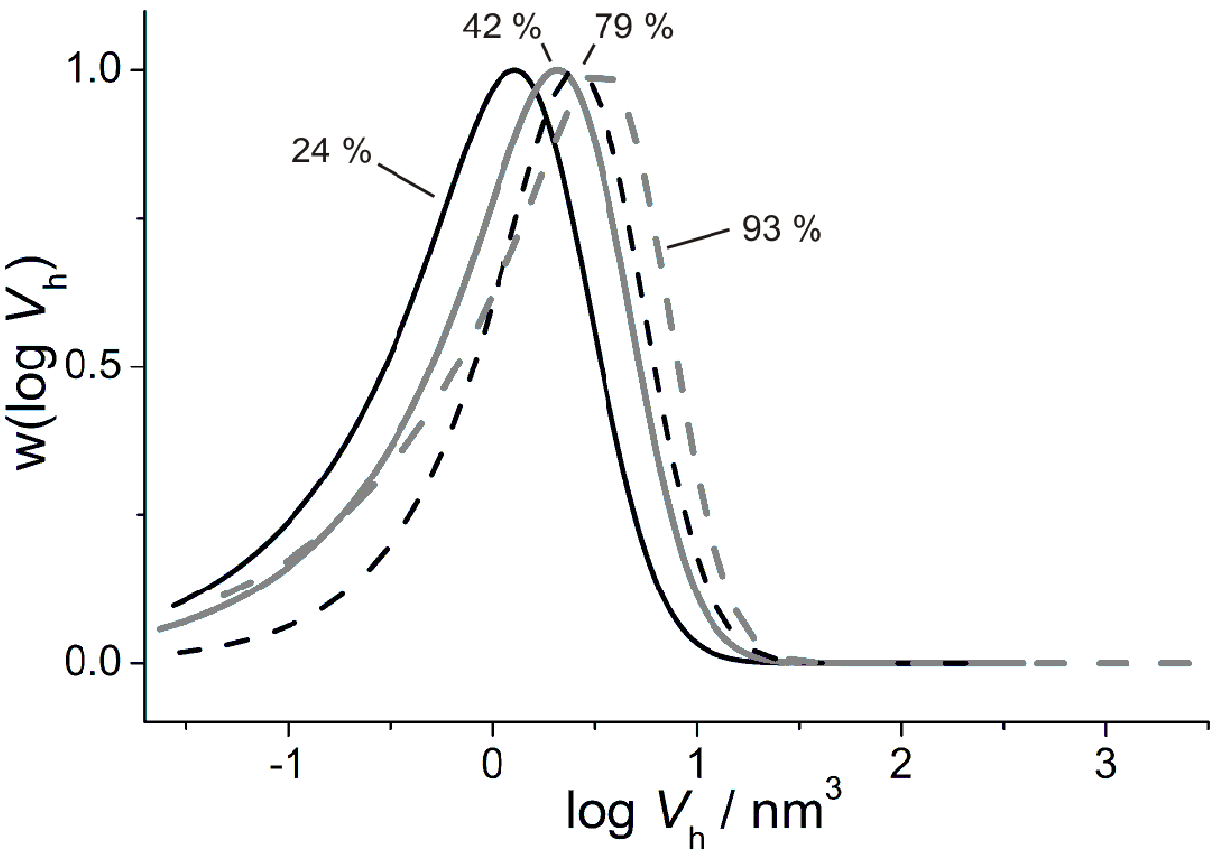

Figure S14. Overlay of hydrodynamic volume distributions at different monomer conversions for the dispersion/emulsion polymerization of DEAAm and styrene initiated by PAA_{23}-SG1 at 112 °C, 30 wt.% solids, $[PAA\text{-}SG1]_0 = 1.24 \times 10^{-2}$ mol L_{aq}^{-1}, and r = 0.10 (Exp. 8).

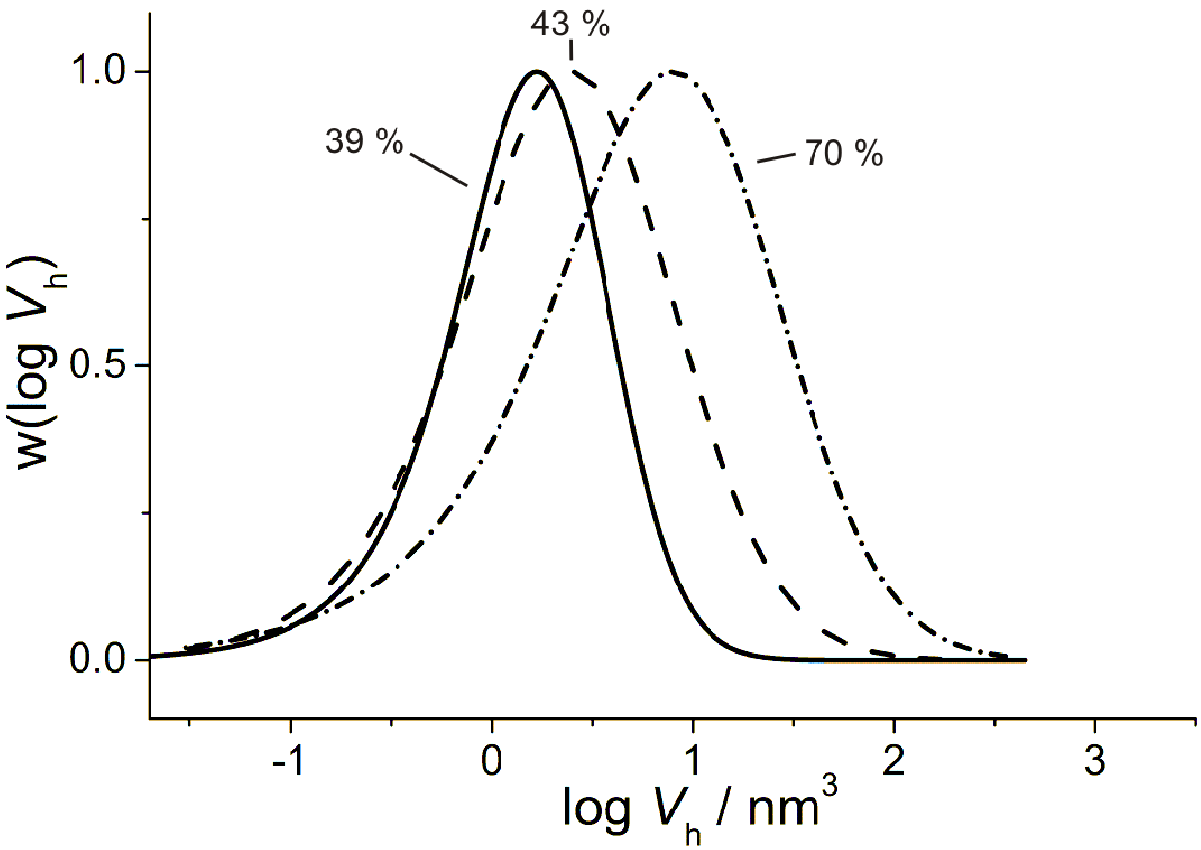

Figure S15. Overlay of hydrodynamic volume distributions at different monomer conversions for the dispersion/emulsion polymerization of DEAAm and styrene initiated by PAA_{24}-SG1 at 112 °C, 30 wt.% solids, $[PAA\text{-}SG1]_0 = 7.3 \times 10^{-3}$ mol L_{aq}^{-1}, and r = 0.10 (Exp. 10).

Correlation between particle size and theoretical degree of polymerization of the PDEAAm block

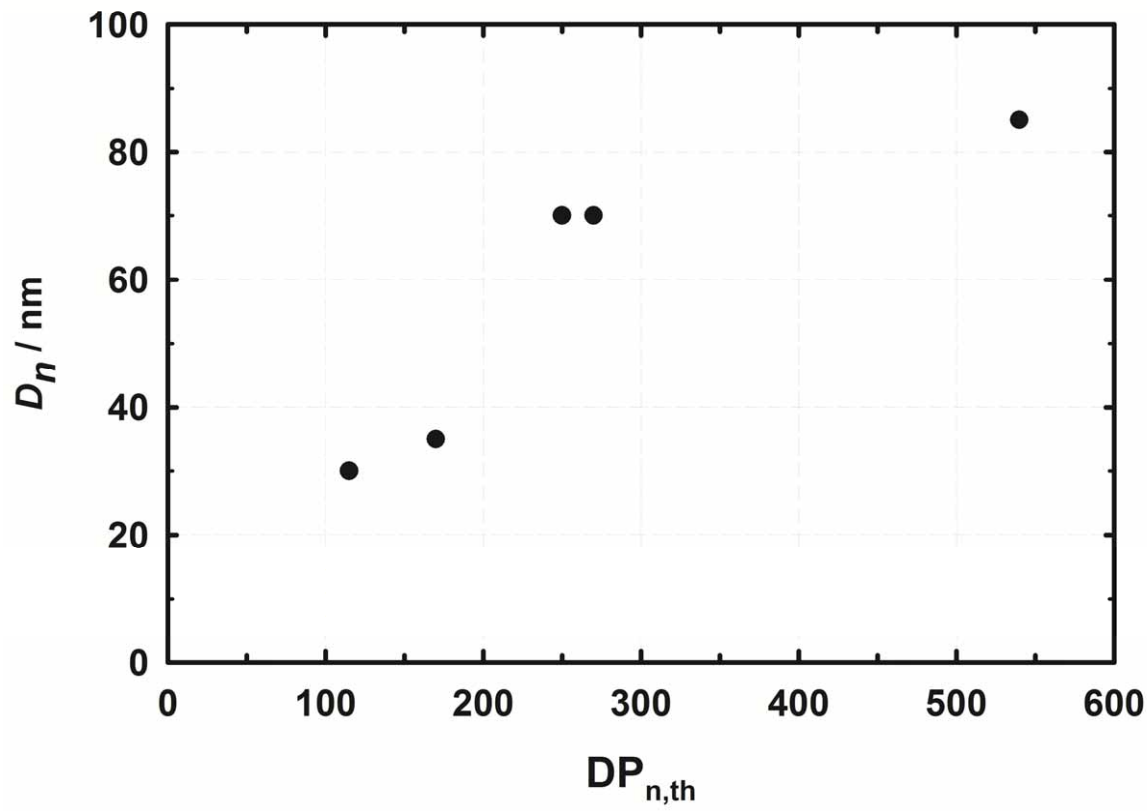

Figure S16. Observed number-average hydrodynamic diameter of the final samples (solids content ~ 20 wt%, exps. 2–7) vs. theoretical degree of polymerization of the PDEAAm block at final conversion.

High-sensitivity scanning differential calorimetry additional data

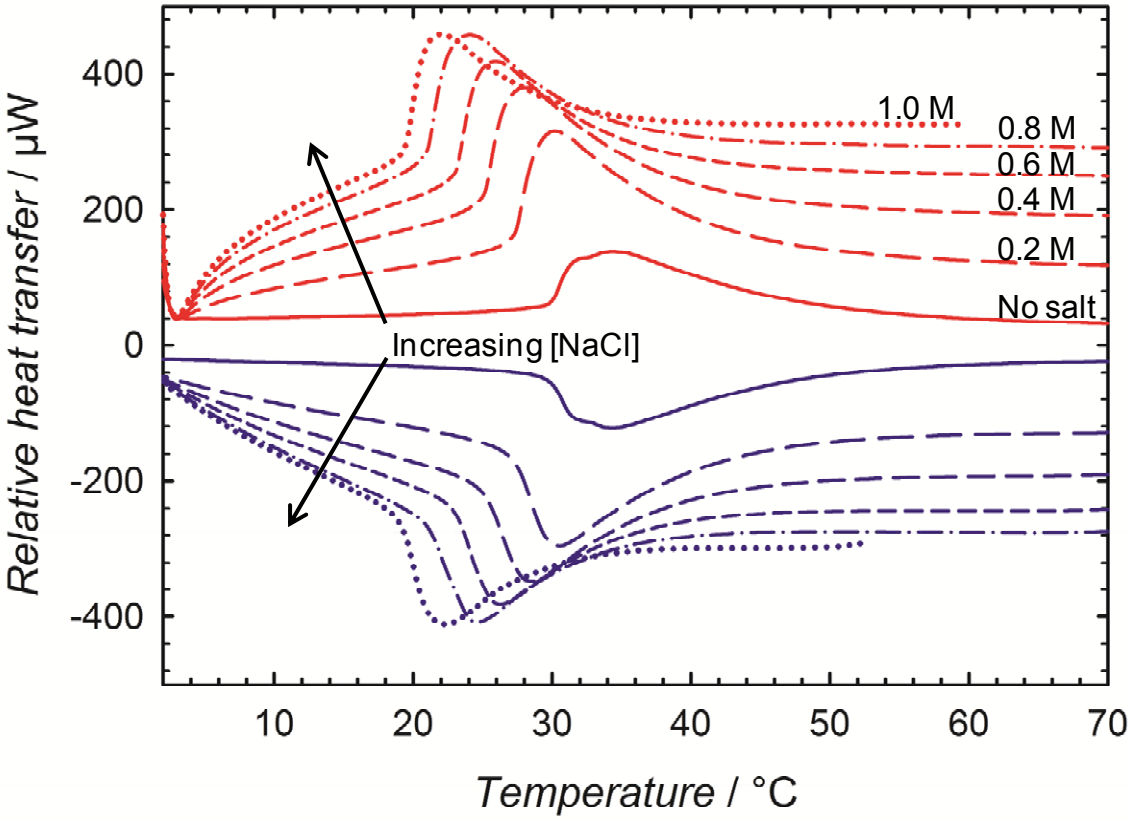

Figure S17. Heat transfer measured by HSDSC on a dialyzed solution of PAA-*b*-PDEAAm copolymers (5 g L^{-1}) at different NaCl concentrations (pH = 6.5). The red curves represent the heating endothermic scans and the blue ones represent the cooling exothermic scans. Heating and cooling rates were 1 °C min^{-1}.

Copolymerization parameters of DEAAm and styrene (S) (physical crosslinking experiment)

To estimate the copolymerization behavior of styrene with DEAAm in exp. 10, we referred to the closest copolymerization system previously published, *i.e.*, copolymerization of styrene with DMAAm in ethanol (the closest solvent to water in the report) at 80 °C (the highest temperature in the report).[11] The reported reactivity ratios were the following: r_S = 1.00 and r_{DMAAm} = 0.19.

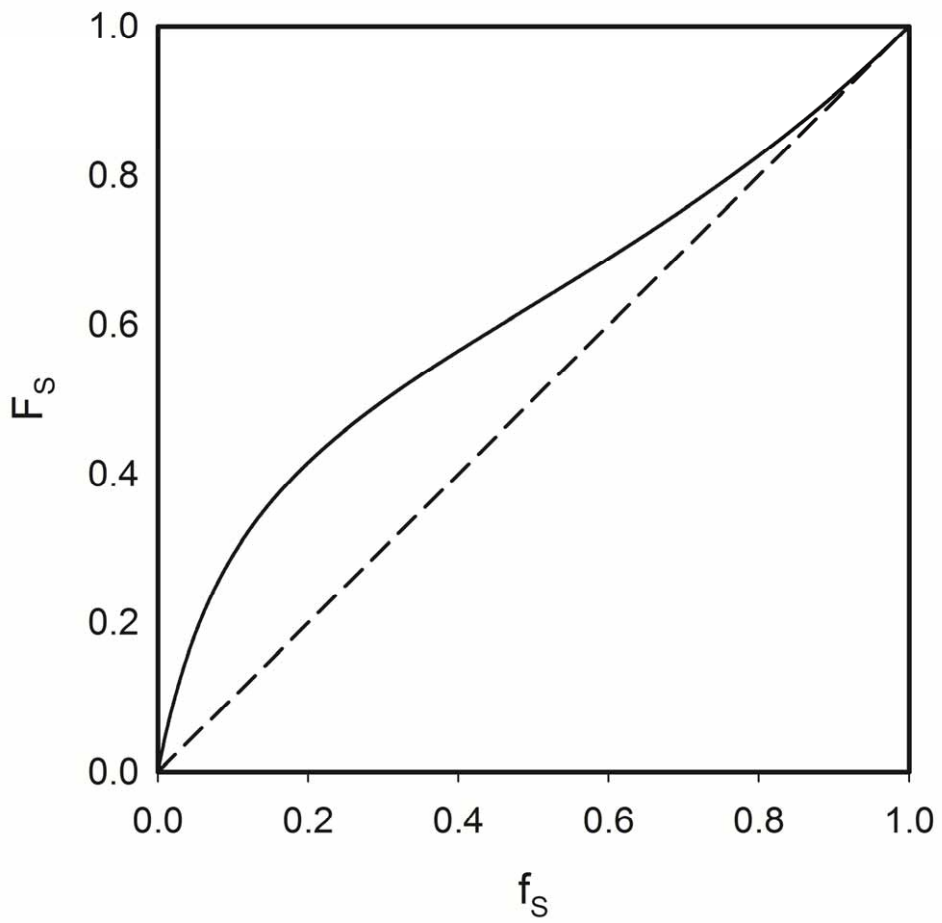

Figure S18. Evolution of the theoretical molar fraction of styrene (S) in a S/DMAAm copolymer vs the molar fraction of S in the comonomer mixture with r_S = 1.00 and r_{DMAAm} = 0.19 (polymerization at 80 °C in ethanol).[11]

References

(1) Kossler, I.; Netopilik, M.; Schulz, G.; Gnauck, R. *Polymer Bulletin* **1982**, *7*, 597-598.

(2) Ioan, S.; Bercea, M.; Ioan, C.; Simionescu, B. C. *Eur. Polym. J.* **1995**, *31*, 85-89.

(3) Bercea, M.; Ioan, C.; Morariu, S.; Ioan, S.; Simionescu, B. C. *Polym.-Plast. Technol. Eng.* **1998**, *37*, 285-294.

(4) Kambe, Y. S. *J. Phys. Chem.* **1968**, *72*, 4104-4110.

(5) Cesteros, L. C.; Katime, I. *Eur. Polym. J.* **1984**, *20*, 237-240.

(6) Tewari, N.; Srivastava, A. K. *Macromolecules* **1992**, *25*, 1013-1016.

(7) Temyanko, E.; Russo, P. S.; Ricks, H. *Macromolecules* **2001**, *34*, 582-586.

(8) Gaborieau, M.; Gilbert, R. G.; Gray-Weale, A.; Hernandez, J. M.; Castignolles, P. *Macromol. Theory Simul.* **2007**, *16*, 13-28.

(9) Berek, D.; Bruessau, R.; Lilge, D.; Mingozzi, T.; Podzimek, S.; Robert, E. In *IUPAC congress/ general assembly*; http://old.iupac.org/projects/posters01/berek01.pdf, Ed., July 2001.

(10) Bruessau, R. J. *Macromol. Symp.* **1996**, *110*, 15-32.

(11) Fujihara, H.; Yoshihara, M.; Maeshima, T. *J. Macromol. Sci. Chem.* **1980**, *14*, 867-877.